

15-A

F 73-14251

C 1

CR-128960

SPACE SHUTTLE GN&C EQUATION DOCUMENT

No. 23

ENERGY DISSIPATION RATE GUIDANCE  
FOR APPROACH PHASE

by

Antonio Elias

(NASA-CR-128960) SPACE SHUTTLE GN AND C  
EQUATION DOCUMENT NO. 23: ENERGY  
DISSIPATION RATE GUIDANCE FOR APPROACH  
PHASE (Massachusetts Inst. of Tech.)

N73-25709

22 p HC \$3.25

CSCL 17G

G3/21

Unclas  
06420

LIBRARY COPY

JUN 1973

JOHNSON SPACE CENTER  
HOUSTON, TEXAS

CHARLES STARK DRAPER  
LABORATORY

MASSACHUSETTS INSTITUTE OF TECHNOLOGY

CAMBRIDGE, MASSACHUSETTS, 02139

SPACE SHUTTLE GN & C EQUATION DOCUMENT

No. 23

Energy Dissipation Rate Guidance  
for Approach Phase

by

Antonio Elias

M.I.T. Charles Stark Draper Laboratory

January 1973

NAS9-10268

for

National Aeronautics and Space Administration

Systems Analysis Branch

Guidance and Control Division

Manned Spacecraft Center, Houston, Texas

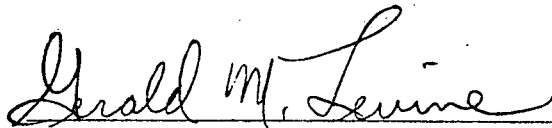
## ACKNOWLEDGEMENT

This report was prepared under DSR Project 55-40800, sponsored by the Manned Spacecraft Center of the National Aeronautics and Space Administration through Contract NAS9-10268.

The publication of this report does not constitute approval by the National Aeronautics and Space Administration of the findings or the conclusions contained therein. It is published only for the exchange and stimulation of ideas.

## FOREWORD

This document is one of a series of candidates for inclusion in a future revision of MSC-04217, "Space Shuttle Guidance, Navigation and Control Design Equations." The enclosed has been prepared under NAS9-10268, Task No. 15-A, "GN & C Flight Equation Specification Support", and applies to function 1 of the Approach Guidance Module (OG6), as defined in MSC-03690, Rev. C, "Space Shuttle Orbiter Guidance, Navigation and Control Software Functional Requirements - Vertical Flight Operations", dated 31 July 1972.

A handwritten signature in cursive script that reads "Gerald M. Levine". The signature is written in dark ink and is positioned above a horizontal line.

Gerald M. Levine, Director  
APOLLO Space Guidance Analysis Division

## TABLE OF CONTENTS

Section 1	Introduction
Section 2	Functional Flow Diagrams
Section 3	Input and Output Variables
Section 4	Description of Equations
Section 5	Detailed Flow Diagrams

## NOMENCLATURE

### Notational Conventions

Lower-case and Greek letters reserved for scalars and vectors

Vector quantities are underlined, e. g.  $\underline{x}$

Components of a vector  $\underline{x}$  are denoted  $x_1, x_2, x_3$

### Symbols

$a_{TAC}$	Azimuth of VORTAC
$d_{INT}$	Distance from touchdown point to final approach plane intersection point
$d_{OM}$	Distance from touchdown point to initiation of landing guidance system
$d_{TAC}$	Distance from touchdown point to VORTAC
$e$	Current vehicle energy
$e_1, e_2, e_3$	Desired vehicle energy at target points
$e_{OLD}$	Value of vehicle energy at previous guidance pass
$\dot{e}$	Current vehicle energy dissipation rate
$\dot{e}_D$	Desired value of vehicle energy dissipation rate
$\dot{e}_{IN}$	Value of $\dot{e}_D$ at which flyover mode is entered
$\dot{e}_{OUT}$	Value of $\dot{e}_D$ at which flyover mode is left

$\dot{e}_{MIN}$	Upper limit of preferred $\dot{e}_D$ region
$\dot{e}_{MAX}$	Lower limit of preferred $\dot{e}_D$ region
$g$	Gravitational constant at sea level
$i$	Current target index variable
$\underline{i}_{DH}$	Unit vector in direction of difference between horizontal components of vehicle and target position vectors
$\underline{i}_{VH}$	Unit vector in direction of horizontal component of velocity w. r. t. touchdown point
$k_E$	Longitudinal channel coefficient
$k_L$	Roll channel coefficient
$k_P$	Vertical (pitch) channel coefficient
$l_1, l_2, l_3$	Horizontal distances from target points at which target switching is to occur
$q$	Current value of dynamic pressure
$q_D$	Desired value of dynamic pressure
$\underline{r}_{RT}$	Vehicle position vector w. r. t. the touchdown point
$\underline{r}_1, \underline{r}_2, \underline{r}_3$	Target points position vectors w. r. t. the touchdown point
$\underline{r}_{DH}$	Vector difference between the horizontal components of vehicle and target position vectors
$\underline{r}_{OLD}$	Vehicle position vector at previous guidance pass
$s_{FO}$	Switch indicating flyover mode is in effect

$s_{FP}$	Switch indicating this is the first pass
$\underline{v}_{RT}$	Vehicle velocity w. r. t. the touchdown point
$\underline{v}_H$	Horizontal projection of velocity vector
$\alpha_{C_{MAX}}$	Maximum permissible angle of attack
$\alpha_{C_{MIN}}$	Minimum permissible angle of attack
$\gamma$	Flight path angle
$\dot{\delta}_{RC}$	Command Rudder Flare deployment angle rate
$\dot{\delta}_{RCL}$	Maximum Rudder Flare deployment angle rate
$\Delta\psi$	Heading error
$\theta_C$	Command vehicle pitch angle
$\theta_{CMINT}$	Minimum pitch angle during transition
$\theta_{CMC}$	Current lower limit for command pitch angle
$\theta_{CM}$	Corrected minimum limit for command pitch angle
$\theta_{C_{MAX}}$	Maximum command pitch angle
$\phi_C$	Command roll angle
$\phi_{C_{MAX}}$	Maximum command roll angle magnitude

Special Notation

Sign ( )	Algebraic sign associated with ( ). Value is +1 or -1, with sign (0) = +1
max ( )	The maximum of all element enclosed in ( )



$\min ( )$  The minimum of all elements enclosed in ( )

$| ( ) |$  Magnitude of ( )

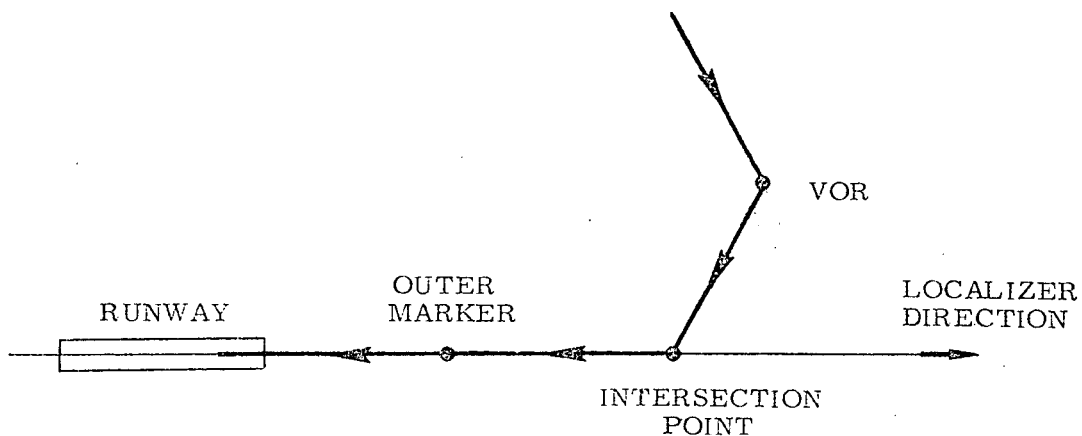
## 1. INTRODUCTION

The Approach-Guidance Routine presented here is designed to take the orbiter vehicle from the end of the Entry Phase (altitude  $\approx 100,000$  ft) to the start of the Final Landing maneuver (altitude  $\approx 7000$  ft). A detailed description of the guidance concept along with simulation results demonstrating its feasibility is given in Ref. (1).

The Approach-Guidance system is a closed-feedback-loop scheme. The vehicle energy is managed by controlling the rate at which energy is dissipated during a straight-in approach flight. Energy dissipation rate is controlled by flying at a constant value of dynamic pressure and varying the vehicle's lift to drag ratio with the Rudder Flare and or other available drag-increasing devices (e.g. body flap).

The complete approach flight consists of straight, fixed-length segments from the vehicle's initial position to the airport's main navigational facility (VOR, TACAN) or a suitable artificial checkpoint, then to a point in the final approach plane (intersection point) where the final flight path is intercepted, then straight towards the runway until the Final Landing Guidance System takes over (Outer Marker). Constant-bank turns link the straight flight segments.

The closed-loop energy management policy automatically compensates for any wind component that may affect the energy dissipation rate of the vehicle.



## 2. FUNCTIONAL FLOW DIAGRAM

The basic information flow for the Approach Guidance Routine is shown in Figure 1. This is based on the guidance concept of Ref. (1).

The guidance task is made up of three independent channels:

1. The pitch angle command is proportional to the difference between the desired and measured dynamic pressure. This command is limited so as to limit the pitch-down during the transition maneuver and the maximum and minimum angles of attack.
2. The desired energy dissipation rate is computed as the ratio of energy-to-be-dissipated to the distance-to-go. The Rudder Flare deployment angle rate is proportional to the difference between the desired and the actual energy dissipation rates. A discrete rate controller is superposed in order to drive the desired dissipation rate to a "preferred" value range.
3. The roll angle command is proportional to the difference between the horizontal velocity direction and the horizontal direction from the vehicle position to the target point.

The three channels guide the vehicle sequentially to three target points. Switchover from one target to the next is made at a predetermined horizontal distance from the current target.

The longitudinal channel (No. 2) is inhibited when the vehicle is initially too close to the first target (desired energy dissipation rate exceeds the maximum available). The guidance is then in "flyover" mode. Target switching is also inhibited in this mode.

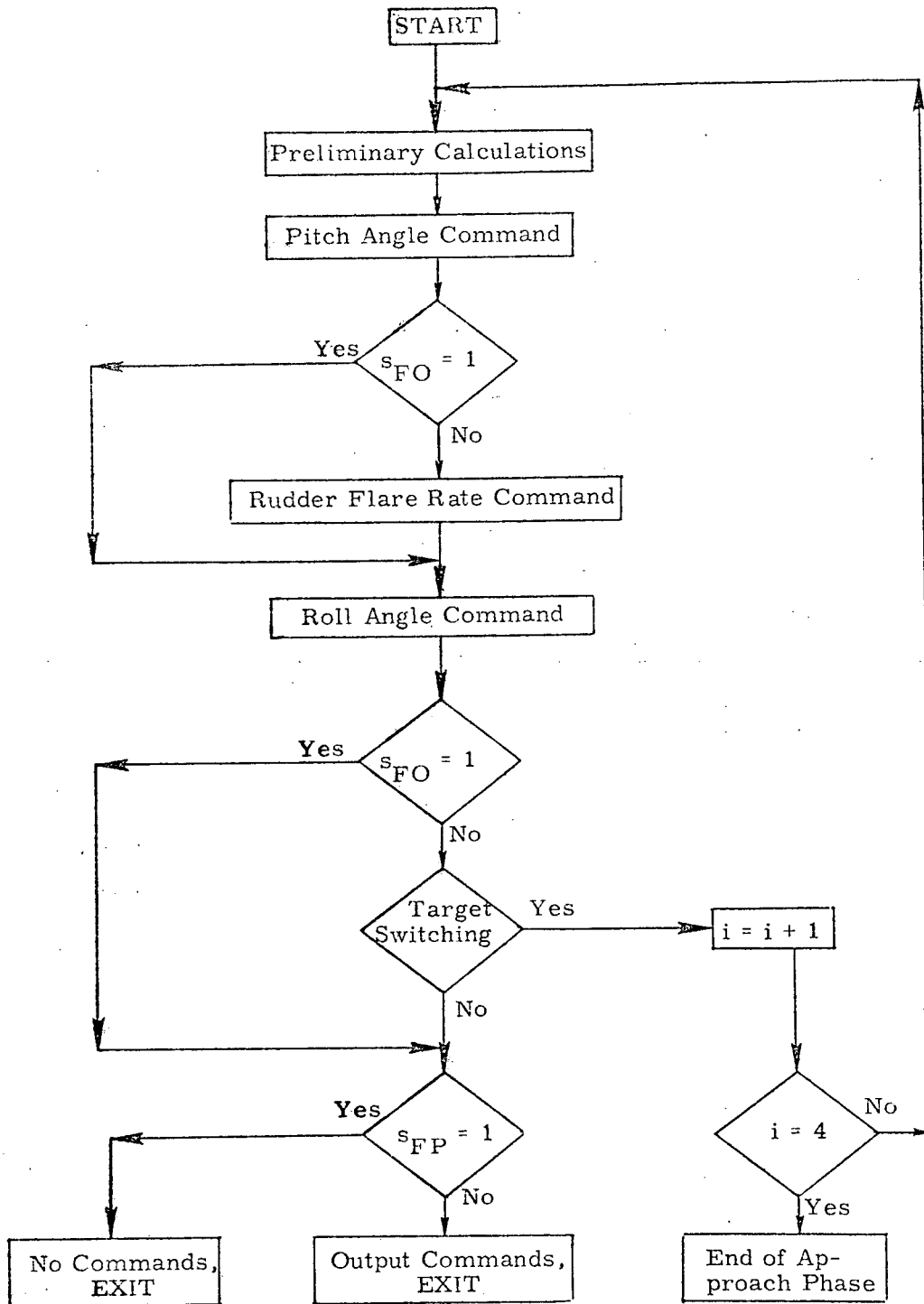


Figure 1. Functional Flow Diagram for Approach Guidance

3. INPUT AND OUTPUT VARIABLES

Input Variables

$\underline{r}_{RT}$  Vehicle position w. r. t. touchdown point (touchdown point coordinates:  
x-up, z-downrange, y-crosstrack)

$\underline{v}_{RT}$  Vehicle velocity w. r. t. touchdown point (touchdown point coordinates)

q Measured value of Dynamic Pressure

Output Variables

$\theta_C$  Pitch angle command

$\dot{\delta}_C$  Rudder Flare deflection angle rate command

$\phi_C$  Roll angle command

#### 4. DESCRIPTION OF EQUATIONS

##### 4.1 Initial Target Calculations

During the initial pass, the target point horizontal position vectors are constructed from their distances to the touchdown point and the VORTAC azimuth w. r. t. the localizer direction:

$$\text{VORTAC: } \underline{r}_1 = (0, -d_{TAC} \sin a_{TAC}, -d_{TAC} \cos a_{TAC})$$

$$\text{Intersection: } \underline{r}_2 = (0, 0, -d_{INT})$$

$$\text{Outer Marker: } \underline{r}_3 = (0, 0, -d_{OM})$$

Also, the following initialization tasks are performed:

1. Flyover mode switch off -  $s_{FO} = 0$ ,
2. Initial pass switch on -  $s_{FP} = 1$ ,
3. Pitch limit = transition pitch limit (it is assumed that the guidance system is initiated with the vehicle flying on the back side of the L/D curve),
4. The target index  $i$  is set to 1 (VORTAC)
5. The "old" values of  $e$  and  $\underline{r}_{RT}$  are set to zero. This makes the back-difference algorithm of section 4.4 invalid during the first pass, so commands are not issued until the second pass.

##### 4.2 Preliminary Calculations

At the beginning of every guidance pass, the flight path angle and horizontal vector from vehicle to target are computed:

$$\gamma = \tan^{-1} \left( v_{RT1} / \sqrt{v_{RT2}^2 + v_{RT3}^2} \right)$$
$$\underline{r}_{DH} = (0, r_{i2} - r_{RT2}, r_{i3} - r_{RT3})$$

##### 4.3 Vertical Channel

The command pitch angle is:

$$\theta_C = k_P (q_D - q)$$

The lower limit for the command pitch angle is the largest of:

1. The current absolute pitch minimum,  $\theta_{CMC}$
2. The pitch angle corresponding to the minimum angle of attack,  $\gamma + \alpha_{CMIN}$ .

The upper limit for the command pitch angle is the pitch angle corresponding to the maximum angle of attack,  $\gamma + \alpha_{CMAX}$ .

The current absolute pitch minimum is set to  $\theta_{CMINT}$  during the transition maneuver, and to an arbitrary low value (e.g. -1 rad.) after the dynamic pressure reaches the desired value for the first time (i.e. at the end of the transition pitch-down).

#### 4.4 Longitudinal Channel

The current vehicle energy is computed from the position and velocity:

$$e = r_{RT1} - (v_{RT} \cdot v_{RT})/2g$$

The current energy dissipation rate is computed as the back-difference:

$$\dot{e} = \frac{e - e_{OLD}}{\sqrt{(r_{RT2} - r_{OLD2})^2 - (r_{RT3} - r_{OLD3})^2}}$$

then the values of  $e_{OLD}$  and  $r_{OLD}$  are updated.

The desired value of the energy dissipation rate is then calculated.

$$\dot{e}_D = (e_i - e) / |r_{DH}|$$

and a Rudder Flare rate is commanded proportional to the difference between desired and actual dissipation rates:

$$\dot{\delta}_{RC} = k_E (\dot{e}_D - \dot{e})$$

this rate is then limited to the  $-\dot{\delta}_{RCL}, \dot{\delta}_{RCL}$  range. This command is overridden if the value of  $e_D$  falls outside of a "preferred" range:

$$\begin{aligned} \text{if } \dot{e}_D > \dot{e}_{MIN}, \dot{\delta}_{RC} &= -\dot{\delta}_{RCL} \\ \text{if } \dot{e}_D < \dot{e}_{MAX}, \dot{\delta}_{RC} &= \dot{\delta}_{RCL} \end{aligned}$$

The "flyover" mode is enabled when  $\dot{e}_D$  is lower than  $\dot{e}_{IN}$ , and is disabled when  $\dot{e}_D$  reaches  $\dot{e}_{OUT}$ . When the "flyover" mode is enabled, the command rudder flare rate is zero.

#### 4.5 Lateral Channel

Two unit vectors are computed:

$$\underline{i}_{VH} = \frac{\underline{v}_{RT}}{|\underline{v}_{RT}|} \quad \text{is in the current vehicle heading direction}$$

$$\underline{i}_{DH} = \frac{\underline{r}_{DH}}{|\underline{r}_{DH}|} \quad \text{is in the direction from the vehicle to the target}$$

The dot product of these vectors is the cosine of the angle difference between the desired and the actual headings. In order to resolve the sign indetermination of the  $\cos^{-1}$  function, the single component of the cross product

$$\underline{i}_{DH} \times \underline{i}_{VH} = i_{DH_2} i_{VH_3} - i_{DH_3} i_{VH_2}$$

is computed. This is the sine of the heading difference, and its sign is used to resolve the indetermination.

This command roll angle is then calculated:

$$\phi_C = k_L \Delta\psi$$

This command is limited to the  $-\phi_{C\text{MAX}}, \phi_{C\text{MAX}}$  range.

#### 4.6 Target Switching

The target index variable, is incremented when the horizontal distance to the current target reaches the target's switching value. When the last target's switching distance is reached, ( $i = 4$ ), the Approach Guidance is terminated. Target switching is inhibited during the "flyover" mode ( $s_{FO} = 1$ ).

Commands are not issued during the first pass.



5. DETAILED FLOW DIAGRAMS

This section contains detailed flow diagrams of the Approach Guidance Routine.

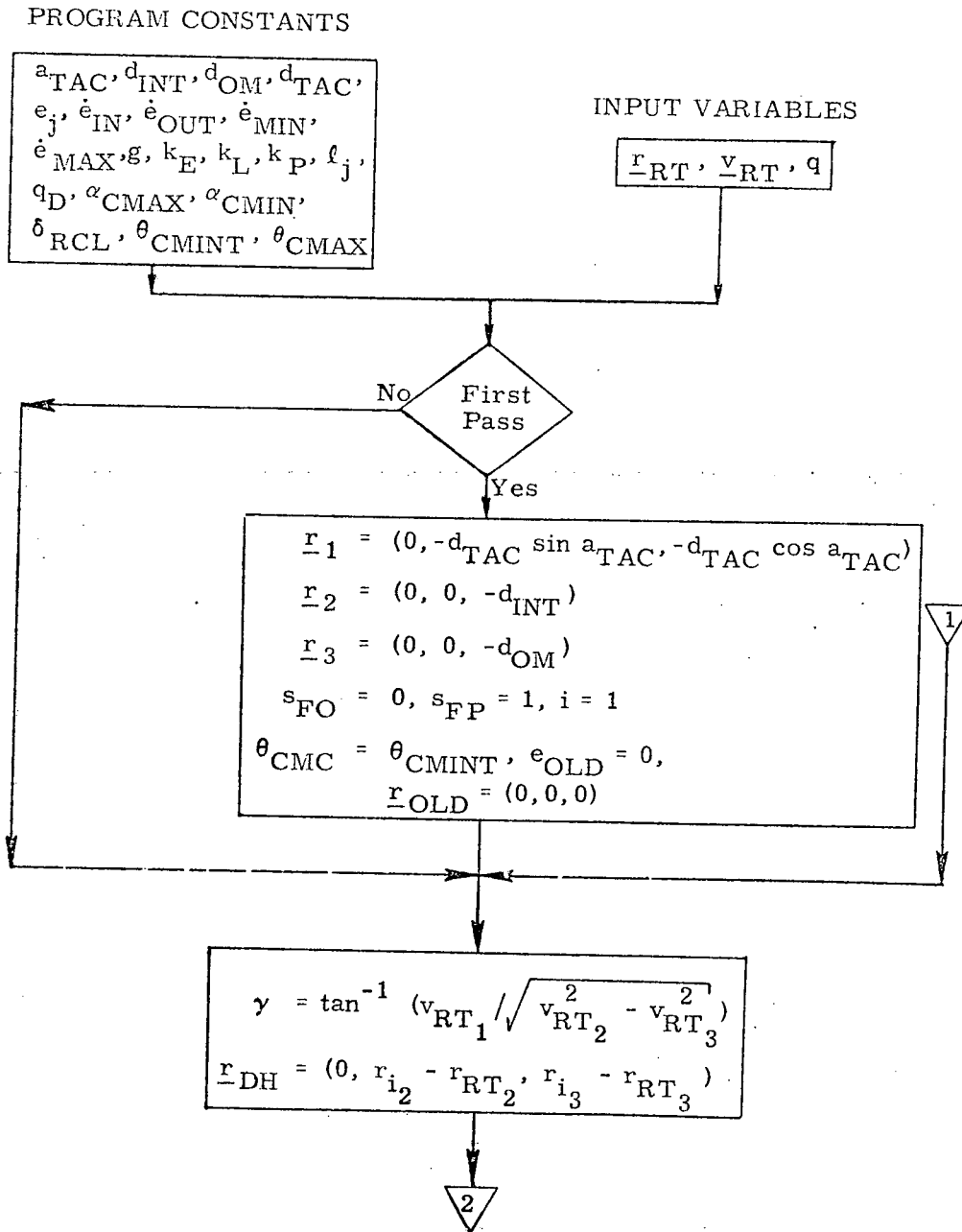


Figure 2a. Approach Guidance Routine, Detailed Flow Diagram

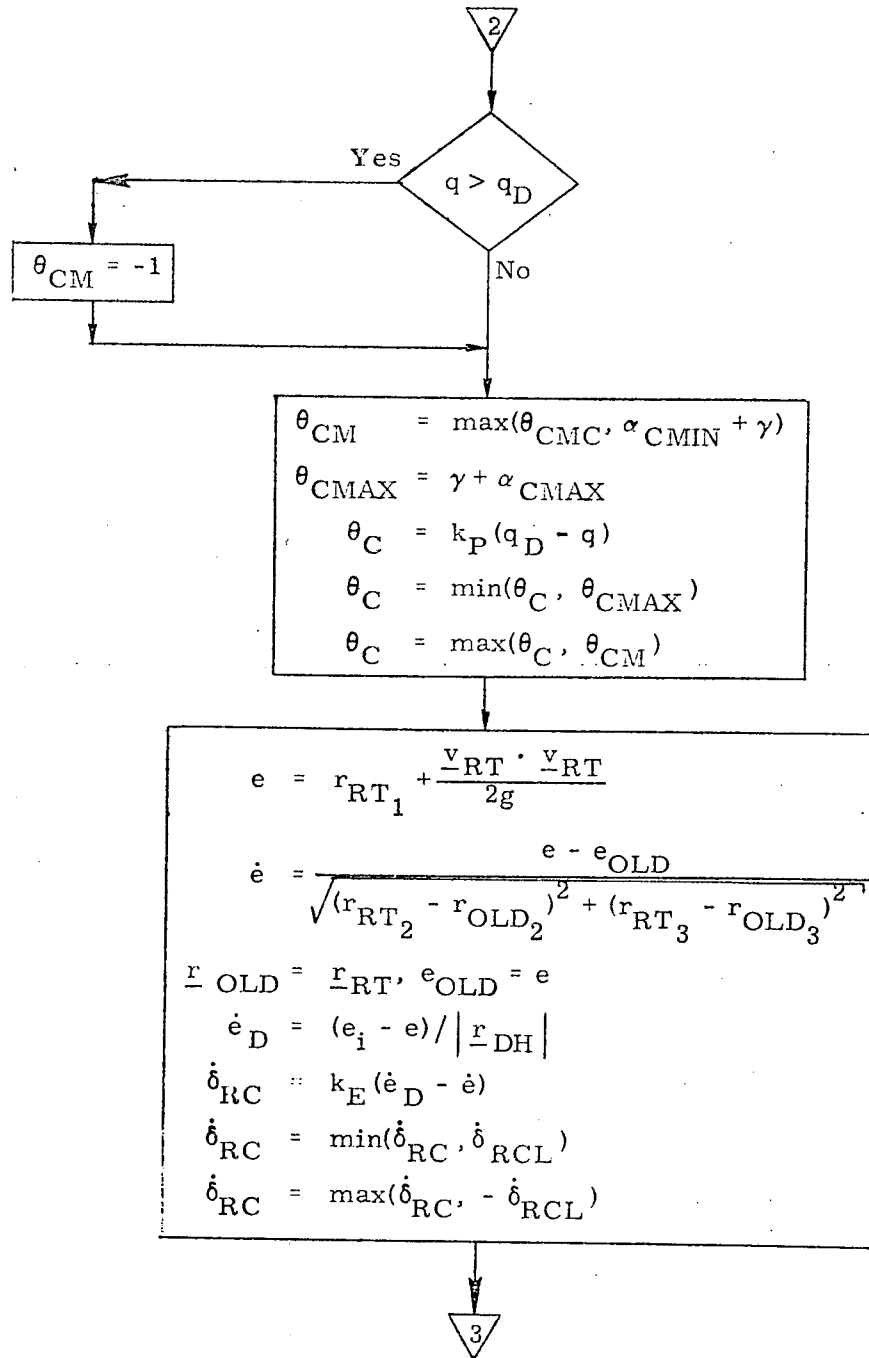


Figure 2b. Approach Guidance Routine,  
Detailed Flow Diagram

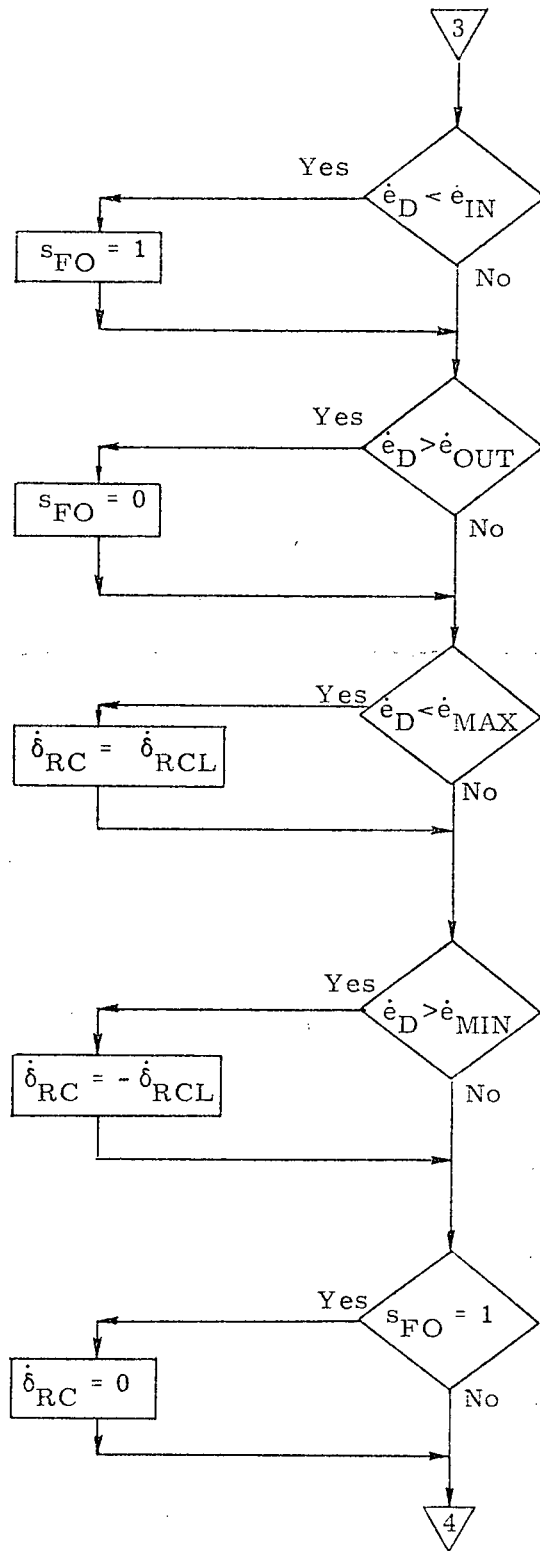


Figure 2c. Approach Guidance Routine, Detailed Flow Diagram

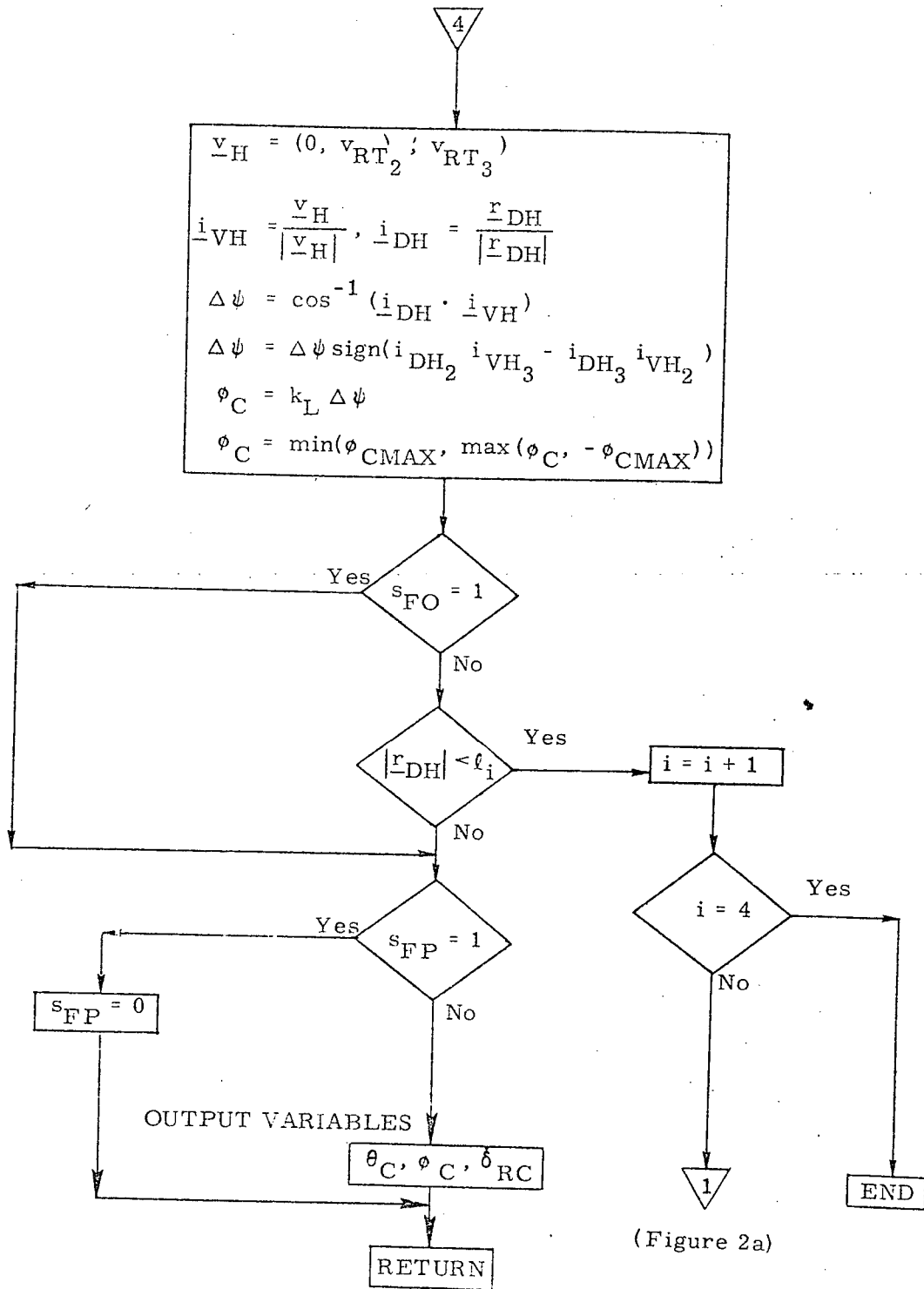


Figure 2d. Approach Guidance Routine,  
Detailed Flow Diagram

## REFERENCES

1. Elias, A., "New Approach Guidance Concept for Shuttle", 23A STS Memo No. 58-72, 4 December 1972, MIT/Draper Laboratory.

DO NOT REPRODUCE

23A SHUTTLE DISTRIBUTION LIST

INTERNAL (82)		EXTERNAL (34)	
<u>23A</u>	(35)	<u>EA2</u>	( 1)
<u>23B</u>	( 2)	W. Bradford	
M. Hamilton		<u>EG</u>	( 1)
J. Kernan		D. Cheatham	
<u>23C</u>	(22)	<u>EG2</u>	(12)
<u>23D</u>	( 1)	K. Cox	
I. Johnson		D. Dyer	
<u>23I</u>	( 2)	E. Kubiak	
R. McKern		F. Elam	
W. Tanner		B. Marcantel	
<u>23N</u>	( 1)	W. Peters	
G. Ogletree		C. Price	
<u>23P</u>	(13)	R. Saldana	
R. Battin		E. Smith	
S. Copps		J. Suddath	
D. Dolan (4)		J. Sunkel	
T. Edelbaum		G. Zacharias	
D. Hoag		<u>EG3</u>	( 1)
L. Larson		J. Lawrence	
R. Larson		<u>EG4</u>	( 1)
R. Millard		P. Sollock	
R. Ragan		<u>EG5</u>	( 1)
N. Sears		C. Manry	
<u>23S</u>	( 3)	<u>EG6</u>	( 1)
G. Edmonds		R. Reid	
P. Felleman		<u>EG7</u>	( 2)
R. White		C. Hackler	
<u>33</u>	( 2)	J. Hanaway	
L. Drane		<u>EG/MIT</u>	( 3)
H. Laning		A. Cook	
<u>35</u>	( 1)	E. Olsson	
M. Johnston		G. Silver	
		<u>FA</u>	( 1)
		H. Tindall	
		<u>FD7</u>	( 1)
		A. Hambleton	
		<u>FM4</u>	( 3)
		B. Cockrell	
		P. Pixley	
		R. Savely	
		<u>FM6</u>	( 2)
		R. Becker	
		P. Shannahan	
		<u>FM7</u>	( 2)
		S. Mann	
		R. Nobles	
		<u>FS6</u>	( 1)
		J. Garman	
		<u>FM</u>	( 1)
		T. Gibson	

Additional for GN&C Equation Documents (21)

G. Levine (10), E. Olsson (5), J. Rogers BC7, E. Smith (5), DL/Technical Document Center (1)